UCSF
UC San Francisco Previously Published Works

## Title
Glioblastoma Therapy Can Be Augmented by Targeting IDH1-Mediated NADPH Biosynthesis

Permalink
https://escholarship.org/uc/item/7bg5h2gz

Journal
Cancer Research, 77(4)

ISSN
0008-5472

Authors
Wahl, Daniel R
Dresser, Joseph
Wilder-Romans, Kari
et al.

Publication Date
2017-02-15

DOI
10.1158/0008-5472.can-16-2008

Peer reviewed

eScholarship.org Powered by the California Digital Library
University of California

Author Manuscript

Author Manuscript

Author Manuscript

Author Manuscript

HHS Public Access

Author manuscript

*Cancer Res*. Author manuscript; available in PMC 2018 February 15.

Published in final edited form as:

*Cancer Res*. 2017 February 15; 77(4): 960–970. doi:10.1158/0008-5472.CAN-16-2008.

# Glioblastoma Therapy Can be Augmented by Targeting IDH1-mediated NADPH Biosynthesis

**Daniel R. Wahl**[1,*], **Joseph Dresser**[1], **Kari Wilder-Romans**[1], **Joshua D. Parsels**[1], **Shuang G. Zhao**[1], **Mary Davis**[1], **Lili Zhao**[2], **Maureen Kachman**[3], **Stefanie Wernisch**[3], **Charles F. Burant**[3], **Meredith A. Morgan**[1], **Felix Y. Feng**[1], **Corey Speers**[1], **Costas A. Lyssiotis**[3,4], and **Theodore S. Lawrence**[1]

[1]Department of Radiation Oncology, University of Michigan, Ann Arbor, MI USA

[2]Department of Biostatistics, University of Michigan, Ann Arbor, MI USA

[3]Department of Internal Medicine, University of Michigan, Ann Arbor, MI USA

[4]Department of Molecular and Integrative Physiology, University of Michigan, Ann Arbor, MI USA

## Abstract

NADPH is a critical reductant needed in cancer cells to fuel the biosynthesis of deoxynucleotides and antioxidants and to sustain stress-survival responses after radiation-induced DNA damage. Thus, one rational strategy to attack cancer cells is to target their heavy reliance on NADPH. Here we report that the isocitrate dehydrogenase IDH1 is the most strongly upregulated NADPH-producing enzyme in glioblastoma (GBM). IDH1 silencing in GBM cells reduced levels of NADPH, deoxynucleotides and glutathione and increased their sensitivity to radiation-induced senescence. Rescuing these metabolic restrictions was sufficient to reverse IDH1-mediated radiosensitization. In a murine xenograft model of human GBM, we found that IDH1 silencing significantly improved therapeutic responses to fractionated radiotherapy, when compared to either treatment alone. In summary, our work offers a mechanistic rationale for IDH1 inhibition as a metabolic strategy to improve the response of GBM to radiotherapy.

## Introduction

Glioblastoma (GBM) is the most common primary intracranial malignancy in adults and is treated with a combination of surgery, radiation and temozolomide(1). Despite intensive treatment, nearly all patients with GBM ultimately succumb to their disease. Temozolomide, which is administered both during and following radiation, is a modest radiosensitizer but may only benefit a small fraction of patients with GBM (2,3). Because most patients with GBM die due to recurrences within the high dose radiation field(4), it is imperative to find strategies to augment or replace temozolomide as the primary radiosensitizer for GBM.

*To whom correspondence should be addressed: dwahl@med.umich.edu.

Felix Y. Feng has received grant funding from Varian Inc. not directly related to this manuscript. The other authors declare no potential conflicts of interest.

Author Manuscript Author Manuscript Author Manuscript Author Manuscript

Aberrant metabolism is a hallmark of cancer and could be a promising target for the selective radiosensitization of GBM (5–7). One of the primary functions of altered metabolism in cancer is to generate NADPH, which carries the reducing potential used to maintain antioxidants and fuel reductive biosynthesis (8). Several NADPH-requiring biomolecules are involved in the radiation response, including glutathione and thioredoxin, which help mitigate the oxidative stress induced by ionizing radiation; and deoxynucleotides, which are needed to repair radiation-induced DNA damage (9). Because altered NADPH metabolism distinguishes GBM from surrounding non-cancerous tissue, and NADPH-requiring biomolecules mitigate radiation-induced cell death, we hypothesized that the inhibition of key NADPH producing enzymes would selectively potentiate the efficacy of radiation therapy for GBM and therefore could improve outcomes for patients with this disease. Herein, we show that isocitrate dehydrogenase 1 (IDH1) is the most upregulated NADPH-producing enzyme in GBM and that its inhibition sensitizes GBM to radiation *in vitro* and *in vivo* by inducing NADPH-dependent cellular senescence.

## Materials and Methods

### Patient Cohorts

Four independent patient cohorts were utilized to analyze the expression of NADPH-producing enzymes in GBM and normal brain tissue(10–13). Oncomine (oncomine.org) was used to calculate the over-expression gene rank of each NADPH-producing enzyme using the log2 median-centered intensity of mRNA transcript levels. Fold changes in transcript levels were calculated with respect to normal brain tissue in each individual patient cohort and analyzed using t tests.

### Cell Culture

U87, A172 and U138 GBM cell lines were obtained directly from and authenticated using short tandem repeat profiling by the American Type Culture Collection in 2015 and used immediately upon receipt. All GBM lines were cultured in Dulbecco's modified Eagle's Medium (DMEM, Gibco) supplemented with 10% fetal bovine serum (Life Technologies), 2 mM L-Glutamine, penicillin and streptomycin (Sigma).

**qPCR—**RNA was isolated from cells using the miRNeasy Mini Kit (QIAGEN) according to the manufacturer's protocol and converted into cDNA using the High-Capacity cDNA Reverse Transcription Kit (ThermoFisher). Real time quantitative PCR was performed using Fast SYBR Green Master Mix on a Quant Studio 6 Flex PCR system (Applied Biosystems). PCR Primers were obtained from Integrated DNA Technologies with the following sequences: IDH1 (CTATGATGGTGACGTGCAGTCG, CCTCTGCTTCTACTGTCTTGCC), IDH2 (AGATGGCAGTGGTGTCAAGGAG, CTGGATGGCATACTGGAAGCAG), IDH3a (TCGGTGTGACACCAAGTGGCAA, TTCGCCATGTCCTTGCCTGCAA), H6PD (GGTGGACCATTACTTAGGCAAGC, CTTCAGCATCCACGGTCTCTTTC), PGD (GTTCCAAGACACCGATGGCAAAC, CACCGAGCAAAGACAGCTTCTC), ME1 (GGAGTTGCTCTTGGTGTTGTGG, GGATAAAGCCGACCCTCTTCCA), ME2 (ATCCTACAGCACAGGCAGAGTG, TGACCTGGTGTAAAGACTCGCC), MTHFD1 (TTGGACAGGCTCCAACGGAGAA,

Author Manuscript Author Manuscript Author Manuscript Author Manuscript

AGAAGTGGTGAGAGCCAGGACA), NNT (GTTGGCACTGATGGGAGGACAT, GTCCAGCATTCTCTGAGTCACC), GAPDH (GTCTCCTCTGACTTCAACAGCG, ACCACCCTGTTGCTGTAGCCAA).

### Immunoblotting

Whole cell lysates were prepared in SDS lysis buffer (10 mM Tris pH 7.4, 2% SDS) supplemented with PhosSTOP phosphatase inhibitor and cOmplete protease inhibitor tablets (Roche) as previously described(14). Antibodies recognizing the following proteins were used: IDH1 (rabbit, D2H1, catalog # 8137, Cell Signaling), GAPDH (rabbit, 14C10, catalog #2118, Cell Signaling), HRP-linked anti-rabbit (goat, catalog #7074, Cell Signaling).

### siRNA and shRNA Studies

Small interfering RNAs (siRNAs) were obtained from Dharmacon and transfected into cells according to the manufacturer's protocol. Briefly, 1–2*$10^5$ cells were plated per well in a 6 well dish and transfected with 5–10 nM siRNA and 5 uL Dharmafect 1 transfection reagent. IDH1 knockdown was maximal 3–4 days following transfection, at which point cells were used for additional experiments. siRNAs used were a 1:1:1:1 pool of the following sequences: IDH1 (UGUCAUAGAUAUCCCGUUU, GCAUAAUGUUGGCGUCAAA, GCUUGUGAGUGGAUGGGUA, CCGCAGGAGAGUUUGGAAU), non-targeting(NT) (UGGUUUACAUGUCGACUAA, UGGUUUACAUGUUGUGUGA, UGGUUUACAUGUUUUCUGA, UGGUUUACAUGUUUUCCUA). Short hairpin RNAs (shRNAs) in the pTRIPZ vector under the control of a tetracycline-inducible promoter were obtained from Dharmacon. Clone #V2THS_217815 was used for IDH1 (mature antisense sequence TTTCGTATGGTGCCATTTG) while control hairpin # RHS4743 (mature antisense sequence CTTACTCTCGCCCAAGCGAGAG) was used as a non-targeting control. Lentiviral production was performed by the University of Michigan Vector Core Facility. Transduced cells were selected with puromycin (1 μg/ml) for one week before further use. Stably transduced cells were treated with doxycycline (1 mg/ml) for 3–4 days to induce knockdown prior to use.

### Mass Spectrometry Sample Preparation

Approximately 2–3*$10^6$ cells per 6 cm plate were washed with distilled $H_2O$ and flash frozen using liquid $N_2$ and stored at −80 °C until analyzed. To each 6 cm plate, 0.5 mL of a mixture of methanol, chloroform and water (8:1:1) containing isotope labeled internal standards was added at 4 °C. Plates were gently agitated to release cells, scraped to homogenize cells, and the resultant mixture quantitatively transferred to a microtube. Microtubes were vortexed, and allowed to incubate at 4 °C for 10 minutes to complete metabolite extraction. Samples were vortexed a second time, and then centrifuged at 14,000 RPM for 10 min in 4 °C. Extraction solvent (100 μL) was transferred to an autosampler vial for LC-MS analysis. A 10 μL aliquot of each sample was analyzed in a separate autosampler vial for quality control.

Author Manuscript Author Manuscript Author Manuscript Author Manuscript

### LC-MS Analysis

GSH/NADP/NADPH analysis was performed on an Agilent system consisting of a 1260 UPLC coupled with a 6520 Quadrupole-Time-of-flight (QTOF) mass spectrometer (Agilent Technologies, Santa Clara, CA). Metabolites were separated on a 150×1mm Luna NH2 Hilic column (Phenomenex, Torrance, CA) using 10 mM ammonium acetate in water, adjusted to pH 9.9 with ammonium hydroxide, as mobile phase A, and acetonitrile as mobile phase B. The flow rate was 0.075 mL/min and the gradient was linear from 20% to 100% A over 15 mins, followed by isocratic elution at 100% A for 5 minutes. The system was returned to starting conditions (20% A) and held there for 10 minutes to allow for column re-equilibration before injecting another sample. The mass spectrometer was operated in ESI-mode according to previously published conditions(15). Nucleotide/Deoxynucleotide analysis was performed on an Agilent system consisting of a 1290 UPLC coupled with a 6490 Triple Quad (QqQ) mass spectrometer (Agilent Technologies, Santa Clara, CA.) Metabolites were separated on a 150×2.1mm Sequant ZIC-cHilic column (EMD Millipore, Billerica, MA ) using 50 mM ammonium acetate in water, adjusted to pH 9.9 with ammonium hydroxide, as mobile phase A, and acetonitrile as mobile phase B. The flow rate was 0.3mL/min and the gradient was linear from 25% to 50% A over 10 mins. The system was returned to starting conditions (25% A) and held there for 10 minutes to allow for column re-equilibration before injecting another sample. The mass spectrometer was operated in negative ion Dynamic MRM mode, with a fragmentor voltage of 380, and cell acceleration voltage of 4. Transitions were determined using the Agilent Optimizer software, and unique mass/retention time/MRM combinations were selected for each metabolite being analyzed. MRM transitions are included in supplemental table 1. Data were processed using MassHunter Quantitative analysis version B.07.00. Metabolites were normalized to the nearest internal standard, and the peak areas were used for differential analysis between groups.

### Clonogenic Survival and Senescence Analysis

Clonogenic assays were performed as described previously(14,16). Briefly, 3–4 days following siRNA transfection or doxycycline-induced shRNA expression, proliferating cells were irradiated with 0–8 Gy and replated at clonal density. After 10–14 days of growth, colonies of 50 or more cells were enumerated and corrected for plating efficiency using unirradiated samples. Cell survival curves were fitted using the linear-quadratic equation. Enhancement ratios were calculated as the ratio of the mean inactivation dose under control conditions divided by the mean inactivation dose under IDH1 knockdown conditions. Cellular senescence was assayed by staining for senescence-associated β-galactosidase according to published methods(17). Following staining, approximately 100 cells per sample were scored by a blinded observer to quantify senescence.

### Xenograft Studies

All procedures involving mice were approved by the University Committee on Use and Care of Animals (UCUCA) at the University of Michigan. C.B-17 SCID mice (male, 4–7 weeks old) were obtained from Envigo and maintained in specific pathogen free conditions. U87 cells ($2*10^6$) carrying a doxycycline-inducible shRNA against IDH1 or control (NT) were

Author Manuscript Author Manuscript Author Manuscript Author Manuscript

resuspended in 1:1 PBS:Matrigel (BD Biosciences) and injected into the bilateral dorsal flanks. Once tumor volumes reached 60–80 $mm^3$, mice were randomized to receive no treatment, doxycycline alone, radiation alone or combined doxycycline and radiation. Doxycyline (2mg/ml) was administered via drinking water and changed daily. Radiation (2 Gy/fraction) was administered over 7 daily fractions on weekdays using a Philips RT250 (Kimtron Medical) unit at a dose rate of ~2 Gy/minute. Dosimetry was performed using an ionization chamber directly traceable to a National Institute of Standards and Technology calibration. Animals were anesthetized with isoflurane and positioned such that the apex of each flank tumor was at the center of a 2.4-cm aperture in the secondary collimator, with the rest of the mouse shielded from radiation(18). Tumor volumes were determined thrice weekly using digital calipers and the formula $(\pi/6)$ (Length $\times$ $Width^2$).

### Statistical Methods

Clonogenic survival, senescence, qPCR and metabolomic data were analyzed by t tests using GraphPad Prism Version 6 with the Holm-Sidak method employed to account for multiple comparisons when appropriate. Growth rates of GBM xenografts were analyzed using a linear mixed effects model on log-transformed tumor volumes. The model included a random intercept and slope to allow each tumor to have its own growth profile. Differences in growth rates between treatment groups were tested through the group-time interaction term in the linear mixed effects model. Additionally, time to tumor tripling was determined for each xenograft by identifying the earliest day on which it was at least three times as large as on the first day of radiation treatment and then estimated by the Kaplan-Meier method and compared using the Log-rank test.

Significance threshold was set at $p<0.05$. These analyses were conducted using SAS (version 9.4, SAS Institute, Cary, NC).

## Results

### Nomination and phenotypic investigation of IDH1 as a target for radiosensitization

To determine whether the enzymes that produce NADPH are differentially expressed in GBM and normal brain, we interrogated four independent clinical data sets that comprehensively analyzed transcript levels of both GBM tissue and normal brain(10–13). IDH1 was the most upregulated NADPH-producing enzyme in three out of the four data sets and was the only enzyme among the top 5% of upregulated genes in each data set (Table 1). Transcript levels of IDH1 were increased up to 4.5-fold compared to normal brain (Figure 1A). We next asked whether radiation further increased the expression of NADPH-producing enzymes in a cell line model of GBM and found that only IDH1 was significantly upregulated following radiation (Figure 1B). This upregulation of IDH1 was confirmed at the protein level (Supplemental Figure 1B–1C), but was less pronounced when a low dose of radiation were used (Supplemental Figure 1D). We also noted increased expression of IDH1 protein following radiation in siRNA-treated cells (Supplemental Figure 1B–1C), possibly due to the outgrowth of cells in which IDH1 was not silenced.

Author Manuscript
Author Manuscript
Author Manuscript
Author Manuscript



Because IDH1 was both the most upregulated NADPH-producing enzyme in GBM and was further upregulated by radiation, we next assessed whether its inhibition could improve the response of GBM to radiation. We chose to investigate this question in three IDH1/2 wild type cell lines with differing P53 mutational status (U87 $P53^{wt}$, A172 $P53^{mut}$, U138 $P53^{mut}$) that were resistant to radiation in preliminary experiments ($SF_{2Gy}$ 0.5–0.7). Knockdown of IDH1 significantly sensitized each of these cell lines to radiation with enhancement ratios between 1.3 and 1.6 (Figure 2A–C, F), which compares favorably to the radiosensitization typically induced by temozolomide(19,20). An independent knockdown strategy using a doxycycline-induced shRNA against IDH1 encoding an antisense sequence distinct from those used in siRNA experiments revealed similar radiosensitization (Figure 2D–F).

## Mechanistic investigation of IDH1-mediated radiosensitization

To determine how IDH1 knockdown radiosensitized GBM, we next analyzed the modes of abrogated replicative capacity encompassed by the clonogenic survival assay. We found only small differences in the induction of apoptosis, necrosis, autophagy and unrepaired DNA double-strand breaks when radiation was combined with IDH1 knockdown (Supplemental Figure 1 and 2A). Similarly, IDH1 knockdown did not affect homologous recombination repair (Supplemental Figure 2B). By contrast, the combination of radiation and IDH1 knockdown induced cellular senescence in more than 60% of cells across multiple GBM lines, which was nearly two-fold higher than radiation treatment alone (Figure 3). The magnitude of senescence increase was similar to the magnitude of radiosensitization induced by IDH1 knockdown, suggesting that increased senescence may be the dominant mechanism of radiosensitization caused by IDH1 knockdown.

Numerous metabolites downstream of IDH1 are related to both the radiation response and the induction of senescence and could therefore be responsible for the IDH1 knockdown-mediated radiosensitization of GBM. We therefore analyzed intracellular metabolite pools following IDH1 knockdown and found up to a 60% depletion of deoxynucleotides and reduced glutathione (GSH), all of which could require IDH1-generated NADPH for their synthesis (Figure 4A–B). In support of this hypothesis, IDH1 knockdown decreased NADPH levels by 50% while simultaneously increasing NADP levels by a similar magnitude (Figures 4C and 4D). Numerous ribonucleotides, which do not require NADPH to be synthesized, were not affected by IDH1 knockdown (Figure 4E), suggesting that these changes were not due to non-specific depletion of metabolite pools. Both control and IDH1 knockdown cells had identical cell cycle profiles, suggesting that observed changes in metabolites are due to restricted NADPH production by IDH1 rather than cell cycle effects (Supplemental Figure 3).

We next asked whether these observed metabolite changes were directly responsible for the IDH1 knockdown-mediated radiosensitization of GBM. Incubation with deoxynucleotide precursors (Nuc) had no effect on the radiosensitivity of control GBM cells but significantly reduced the radiosensitivity of cells in which IDH1 had been knocked down (Figure 5A–B). Similarly, incubation with the antioxidant precursor N-acetyl cysteine (NAC) significantly reduced the radiosensitivity of GBM cells in which IDH1 had been knocked down, but did not significantly affect control cells (Figure 5C–D). Nuc and NAC each rescued

Author Manuscript Author Manuscript Author Manuscript Author Manuscript

approximately 80–90% of the radiosensitization induced by IDH1 knockdown (Figure 5B and 5D), which suggests that these agents may be acting through overlapping mechanisms, presumably the repletion of NADPH-dependent metabolites. Similarly, Nuc or NAC incubation significantly reversed the accelerated induction of senescence that occurs when radiation is combined with knockdown of IDH1 (Figure 5E). Indeed, Nuc or NAC rescued nearly 90% of increased senescence, consistent with the magnitude of rescue seen in clonogenic survival assays.

### *In vivo* studies of IDH1 knockdown and radiation

To determine whether combining radiation and IDH1 knockdown had similar beneficial anti-GBM effects *in vivo*, we established flank xenografts using a U87 cell line carrying a doxycycline-inducible shRNA directed against IDH1 (i-shIDH1, Figure 6). An inducible knockdown model was chosen rather than a stable shRNA knockdown or CRISPR/Cas9 knockout because it allowed for initial tumor growth to occur with intact IDH1 thereby better modeling a therapeutic intervention. A flank model was used due to the variable CNS penetrance of doxycycline(21,22). Once tumors were 60–80 $mm^3$ in size, animals were randomized into four treatment groups: (1) radiation alone, (2) doxycycline alone, (3) combined radiation and doxycycline and (4) untreated (Figure 6A). Both radiation alone and doxycycline alone significantly slowed tumor growth compared to untreated tumors as analyzed using a linear mixed effects model ($p<0.005$, Figure 6B). Combined doxycycline and radiation significantly slowed tumor growth compared to either treatment alone ($p<0.005$, Figure 6B). Furthermore, combined radiation and doxycycline treatment significantly and supradditively increased the time to tumor tripling (median 21 days) compared to radiation alone (14 days), doxycycline alone (12 days) or no treatment (9 days, Figure 6C). As a control for off target doxycycline effects, we also investigated U87 xenografts carrying an inducible non-targeting shRNA (i-shNT). While radiation maintained its ability to slow tumor growth in this model, doxycycline did not noticeably slow tumor growth on its own or in combination with radiation (Supplemental Figure 4A). Immunoblotting confirmed that administration of doxycycline had the intended effects on IDH1 expression in both i-shIDH1 and i-shNT xenografts (Figure 6D and Supplemental Figure 4B). While average knockdown efficiency was approximately 60%, there was some heterogeneity between tumors as expected for polyclonal cellular populations.

## Discussion

In this study, we have shown that wild type IDH1 is a promising new target for the radiosensitization of GBM. IDH1 is the most upregulated NADPH-producing enzyme in GBM compared to normal brain tissue and is further upregulated following radiation. Knockdown of IDH1 using two independent genetic approaches sensitizes multiple GBM cell lines to radiation by potentiating radiation-induced senescence. IDH1 knockdown depletes NADPH and NADPH-dependent metabolites including deoxynucleotides and glutathione and their supplementation rescues the radiosensitization and accelerated radiation-induced senescence that accompanies IDH1 knockdown. These results are recapitulated *in vivo* where the combination of IDH1 knockdown and radiation significantly slows GBM xenograft growth compared to either intervention in isolation. Together, these

Author Manuscript Author Manuscript Author Manuscript Author Manuscript

findings indicate that GBMs meet their NADPH demands by upregulating IDH1 and that inhibition of this cancer-specific metabolic adaptation can form the basis of effective combination therapies for GBM.

The strategy of combining radiation and IDH1 inhibition utilizes knowledge from the growing field of cancer metabolism to build upon the long and successful history of combining antimetabolites with radiation(23). Older combinations using classical antimetabolites remain the standard-of-care treatment for many locally advanced malignancies(24) and have recently shown clinical promise in the context of GBM(25). The antimetabolites currently used with radiation inhibit either the folate cycle or ribonucleotide reductase, which causes impaired deoxynucleotide synthesis, aberrant repair of radiation-induced double stranded DNA breaks and enhanced cytotoxicity(24). While targeting either deoxynucleotide synthesis or antioxidant regeneration in combination with radiation can be effective, both strategies can be associated with dose-limiting toxicity due to normal tissue effects, presumably because both cancers and normal tissues require these enzymes to mitigate radiation-induced ROS and double strand DNA breaks(26,27). This lack of selectivity is a major limitation of current antimetabolite therapy but may not apply to the inhibition of IDH1.

While the *outputs* of the pathways generating deoxynucleotides and antioxidants are similarly required across cell types, there is increasing evidence that the *inputs* to these pathways may differ between cell types, which could allow for therapeutic selectivity. NADPH is required for both antioxidant regeneration and the generation of deoxynucleotides and can be generated from several metabolic pathways. The oxidative pentose phosphate cycle (PPC) is considered the main source of NADPH in mammalian cells, but recent studies suggest that other sources of NADPH may predominate in certain contexts(28). Methylene tetrahydrofolate dehydrogenase enzymes in the folate cycle appear to be major producers of NADPH in some cell types, while malic enzyme 1 (ME1) plays an important role in differentiated adipocytes and pancreatic cancer(29–31). There is increasing evidence that IDH1 may be a dominant producer of NADPH in high grade gliomas. Indeed, IDH1 has a higher maximal enzymatic activity than other NADPH-producing enzymes in patient-derived GBM tissue(32). Furthermore, our data indicate that IDH1 is the most differentially expressed NADPH producing enzyme in GBM compared to normal brain tissue. Thus, our proposed strategy of treating GBM with combined IDH1 inhibition and radiation may achieve a selectivity not seen with the inhibition of ribonucleotide reductase or the folate cycle due to the preferential use of IDH1 as an NADPH source in GBM.

Our study fits well in the context of prior work that has investigated the relationship between NADPH production and radiation, which has focused on the pentose phosphate cycle (PPC). Indeed, Chinese Hamster Ovary cells lacking glucose 6 phosphate dehydrogenase, the rate limiting step of the oxidative PPC, are approximately 50% more sensitive to radiation compared to controls due to an inability to maintain reduced glutathione levels(33,34). Consistent with these findings, flux through the oxidative PPC increases 3–5 fold after radiation in CHO and A549 lung cancer cells, although these changes were only seen after administration of extremely high doses of approximately 50 Gy(34,35). Conventional doses of radiation (5–8 Gy) produced minimal changes in PPC activity in normal human

Author Manuscript Author Manuscript Author Manuscript Author Manuscript

lymphocytes unless they were also subjected to hypoxia(36), which suggests that other NADPH-producing pathways could be important in the context of radiation. IDH1 and IDH2 have also been implicated in the cellular redox response and their deletion can increase ROS levels and radiation sensitivity in several *in vitro* cell line models of cancer (37–39). Our results are consistent with these findings and extend them to show selectivity for GBM, *in vivo* efficacy and that IDH1 supplies reducing potential for the generation of deoxynucleotides in addition to antioxidants, both of which protect GBM against the radiation response.

Our conclusion that the radiosensitization of GBMs by IDH1 knockdown is primarily due to the induction of accelerated cellular senescence also fits well within the current literature. Both deoxynucleotide and antioxidant depletion induce accelerated senescence in the absence of radiation (40,41). Similarly, radiation often causes GBMs to lose replicative capacity by inducing senescence rather than inducing apoptosis or other mechanisms of cell death (42). Given that metabolic rescue with deoxynucleotide and antioxidant precursors reverses both IDH1-mediated radiosensitization and accelerated senescence, our working model is that IDH1 knockdown depletes deoxynucleotides and antioxidants, which causes accelerated senescence when combined with radiation and leads to radiosensitization (Figure 6E).

Our study focuses on the interaction of radiation with wild type IDH1 in GBM. A small subset of GBMs exhibit a monoallelic point mutation in the active site of IDH1 that confers a neomorphic enzymatic activity in which mutant IDH1 catalyzes the conversion of α-ketoglutarate to (D)-2-hydroxyglutarate(43–45). Patients with this mutation exhibit DNA and histone hypermethylation and have an improved prognosis, while preclinical models of IDH1 mutant tumors suggest that they have depleted NADPH-dependent antioxidants and an increased sensitivity to radiation(46–50). Tumor tissue from patients with IDH1 mutated gliomas exhibit approximately one-half of the maximal IDH1-catalyzed NADPH production as IDH wild type GBMs, consistent with a monoallelic mutation(32). Thus, the inhibition of wild type IDH1 in patients with IDH1 wild type GBMs could improve their treatment responsiveness and lead to improved survival more on par with patients with IDH1 mutant tumors. Even when the IDH1 mutation is present, the single remaining allele of non-mutated IDH1 encodes a wild type enzyme whose maximal capacity has the potential to be a major producer of NADPH(32). Therefore, we anticipate that the strategy of wild type IDH1 inhibition could be efficacious both for patients with wild type or mutant IDH1 GBMs.

Together, our results show that targeting IDH1 could be an efficacious and selective metabolic strategy to abrogate radiation resistance in GBM by affecting numerous nodes of reductive biosynthesis. This strategy marries the successful paradigm of combining classical antimetabolites and radiation with emerging knowledge from the field of cancer metabolism and provides a strong rationale to develop IDH1-targeted therapeutics and study other potential combinations of metabolic pathway inhibition with radiation. We are now taking several steps to move these studies towards clinical translation including; the investigation of IDH1 inhibition in patient-derived xenografts that encompass the known molecular subtypes of GBM, the integration of IDH1 inhibition with temozolomide and radiation, and the development of novel pharmacologic inhibitors of IDH1. We anticipate that the results of

Author Manuscript Author Manuscript Author Manuscript Author Manuscript

these studies will lead to therapeutic advances that will improve the dismal outcomes currently seen for patients with GBM.

## Supplementary Material

Refer to Web version on PubMed Central for supplementary material.

## Acknowledgments

This work was supported by the Taubman Foundation and the National Cancer Institute of the National Institutes of Health under award number P30CA046592. This work also utilized Metabolomics Core Services supported by grant U24 DK097153 of NIH Common Funds Project to the University of Michigan.

We would like to thank the University of Michigan Metabolomics and Vector Cores for their support and technical assistance.

## References

1. Stupp R, Hegi ME, Mason WP, Van den Bent MJ, Taphoorn MJ, Janzer RC, et al. Effects of radiotherapy with concomitant and adjuvant temozolomide versus radiotherapy alone on survival in glioblastoma in a randomised phase III study: 5-year analysis of the EORTC-NCIC trial. The Lancet Oncology. 2009:10.
2. Hegi ME, Diserens AC, Gorlia T, Hamou MF, de Tribolet N, Weller M, et al. MGMT gene silencing and benefit from temozolomide in glioblastoma. The New England journal of medicine. 2005; 352(10):997–1003. [PubMed: 15758010]
3. Carlson BL, Grogan PT, Mladek AC, Schroeder MA, Kitange GJ, Decker PA, et al. Radiosensitizing effects of temozolomide observed in vivo only in a subset of O6-methylguanine-DNA methyltransferase methylated glioblastoma multiforme xenografts. International journal of radiation oncology, biology, physics. 2009; 75(1):212–9.
4. Brandes AA, Tosoni A, Franceschi E, Sotti G, Frezza G, Amista P, et al. Recurrence pattern after temozolomide concomitant with and adjuvant to radiotherapy in newly diagnosed patients with glioblastoma: correlation With MGMT promoter methylation status. Journal of clinical oncology: official journal of the American Society of Clinical Oncology. 2009; 27(8):1275–9. [PubMed: 19188675]
5. Hanahan D, Weinberg RA. Hallmarks of cancer: the next generation. Cell. 2011; 144(5):646–74. [PubMed: 21376230]
6. Mashimo T, Pichumani K, Vemireddy V, Hatanpaa Kimmo J, Singh Dinesh K, Sirasanagandla S, et al. Acetate Is a Bioenergetic Substrate for Human Glioblastoma and Brain Metastases. Cell. 159(7): 1603–14.
7. Venneti S, Dunphy MP, Zhang H, Pitter KL, Zanzonico P, Campos C, et al. Glutamine-based PET imaging facilitates enhanced metabolic evaluation of gliomas in vivo. Science translational medicine. 2015; 7(274):274ra17.
8. Ward PS, Thompson CB. Metabolic reprogramming: a cancer hallmark even warburg did not anticipate. Cancer Cell. 2012; 21(3):297–308. [PubMed: 22439925]
9. Spitz DR, Azzam EI, Li JJ, Gius D. Metabolic oxidation/reduction reactions and cellular responses to ionizing radiation: a unifying concept in stress response biology. Cancer metastasis reviews. 2004; 23(3–4):311–22. [PubMed: 15197331]
10. Shai R, Shi T, Kremen TJ, Horvath S, Liau LM, Cloughesy TF, et al. Gene expression profiling identifies molecular subtypes of gliomas. Oncogene. 2003; 22(31):4918–23. [PubMed: 12894235]
11. Sun L, Hui AM, Su Q, Vortmeyer A, Kotliarov Y, Pastorino S, et al. Neuronal and glioma-derived stem cell factor induces angiogenesis within the brain. Cancer Cell. 2006; 9(4):287–300. [PubMed: 16616334]
12. Murat A, Migliavacca E, Gorlia T, Lambiv WL, Shay T, Hamou MF, et al. Stem cell-related “self-renewal” signature and high epidermal growth factor receptor expression associated with

Author Manuscript Author Manuscript Author Manuscript Author Manuscript

resistance to concomitant chemoradiotherapy in glioblastoma. Journal of clinical oncology: official journal of the American Society of Clinical Oncology. 2008; 26(18):3015–24. [PubMed: 18565887]

13. TCGA. TCGA Brain Analysis. 2013. http://cancergenome.nih.gov/. <http://cancergenome.nih.gov/>
14. Morgan MA, Parsels LA, Kollar LE, Normolle DP, Maybaum J, Lawrence TS. The combination of epidermal growth factor receptor inhibitors with gemcitabine and radiation in pancreatic cancer. Clinical cancer research: an official journal of the American Association for Cancer Research. 2008; 14(16):5142–9. [PubMed: 18698032]
15. Lorenz MA, Burant CF, Kennedy RT. Reducing time and increasing sensitivity in sample preparation for adherent mammalian cell metabolomics. Analytical chemistry. 2011; 83(9):3406–14. [PubMed: 21456517]
16. Lawrence TS. Ouabain sensitizes tumor cells but not normal cells to radiation. International journal of radiation oncology, biology, physics. 1988; 15(4):953–8.
17. Debacq-Chainiaux F, Erusalimsky JD, Campisi J, Toussaint O. Protocols to detect senescence-associated beta-galactosidase (SA-[beta]gal) activity, a biomarker of senescent cells in culture and in vivo. Nat Protocols. 2009; 4(12):1798–806. [PubMed: 20010931]
18. Kausar T, Schreiber JS, Karnak D, Parsels LA, Parsels JD, Davis MA, et al. Sensitization of Pancreatic Cancers to Gemcitabine Chemoradiation by WEE1 Kinase Inhibition Depends on Homologous Recombination Repair. Neoplasia (New York, NY). 2015; 17(10):757–66.
19. Choi EJ, Cho BJ, Lee DJ, Hwang YH, Chun SH, Kim HH, et al. Enhanced cytotoxic effect of radiation and temozolomide in malignant glioma cells: targeting PI3K-AKT-mTOR signaling, HSP90 and histone deacetylases. BMC Cancer. 2014; 14:17. [PubMed: 24418474]
20. Chakravarti A, Erkkinen MG, Nestler U, Stupp R, Mehta M, Aldape K, et al. Temozolomide-mediated radiation enhancement in glioblastoma: a report on underlying mechanisms. Clinical cancer research: an official journal of the American Association for Cancer Research. 2006; 12(15):4738–46. [PubMed: 16899625]
21. Andersson H, Alestig K. The penetration of doxycycline into CSF. Scandinavian journal of infectious diseases Supplementum. 1976; (9):17–9. [PubMed: 1070143]
22. Nau R, Sörgel F, Eiffert H. Penetration of Drugs through the Blood-Cerebrospinal Fluid/Blood-Brain Barrier for Treatment of Central Nervous System Infections. Clinical Microbiology Reviews. 2010; 23(4):858–83. [PubMed: 20930076]
23. Vander Heiden MG. Targeting cancer metabolism: a therapeutic window opens. Nature reviews Drug discovery. 2011; 10(9):671–84. [PubMed: 21878982]
24. Wahl DR, Lawrence TS. Integrating chemoradiation and molecularly targeted therapy. Advanced drug delivery reviews. 2015
25. Kim MM, Camelo-Piragua S, Schipper M, Tao Y, Normolle D, Junck L, et al. Gemcitabine Plus Radiation Therapy for High-Grade Glioma: Long-Term Results of a Phase 1 Dose-Escalation Study. International journal of radiation oncology, biology, physics. 2016; 94(2):305–11.
26. Eisbruch A, Shewach DS, Bradford CR, Littles JF, Teknos TN, Chepeha DB, et al. Radiation concurrent with gemcitabine for locally advanced head and neck cancer: a phase I trial and intracellular drug incorporation study. Journal of clinical oncology: official journal of the American Society of Clinical Oncology. 2001; 19(3):792–9. [PubMed: 11157033]
27. Mitchell JB, Cook JA, DeGraff W, Glatstein E, Russo A. Glutathione modulation in cancer treatment: will it work? International journal of radiation oncology, biology, physics. 1989; 16(5): 1289–95.
28. Patra KC, Hay N. The pentose phosphate pathway and cancer. Trends in biochemical sciences. 2014; 39(8):347–54. [PubMed: 25037503]
29. Liu L, Shah S, Fan J, Park JO, Wellen KE, Rabinowitz JD. Malic enzyme tracers reveal hypoxia-induced switch in adipocyte NADPH pathway usage. Nat Chem Biol. 2016; 12(5):345–52. [PubMed: 26999781]
30. Son J, Lyssiotis CA, Ying H, Wang X, Hua S, Ligorio M, et al. Glutamine supports pancreatic cancer growth through a KRAS-regulated metabolic pathway. Nature. 2013; 496(7443):101–5. [PubMed: 23535601]

Author Manuscript Author Manuscript Author Manuscript Author Manuscript


31. Fan J, Ye J, Kamphorst JJ, Shlomi T, Thompson CB, Rabinowitz JD. Quantitative flux analysis reveals folate-dependent NADPH production. Nature. 2014; 510(7504):298–302. [PubMed: 24805240]
32. Bleeker FE, Atai NA, Lamba S, Jonker A, Rijkeboer D, Bosch KS, et al. The prognostic IDH1( R132 ) mutation is associated with reduced NADP+-dependent IDH activity in glioblastoma. Acta neuropathologica. 2010; 119(4):487–94. [PubMed: 20127344]
33. Tuttle S, Stamato T, Perez ML, Biaglow J. Glucose-6-phosphate dehydrogenase and the oxidative pentose phosphate cycle protect cells against apoptosis induced by low doses of ionizing radiation. Radiation research. 2000; 153(6):781–7. [PubMed: 10825753]
34. Tuttle SW, Varnes ME, Mitchell JB, Biaglow JE. Sensitivity to chemical oxidants and radiation in CHO cell lines deficient in oxidative pentose cycle activity. International journal of radiation oncology, biology, physics. 1992; 22(4):671–5.
35. Varnes, ME., Biaglow, JE. Role of Peroxidase in Stimulation of the Pentose Cycle of A549 Cells by Aerobic Irradiation. In: Cerutti, PA.Nygaard, OF., Simic, MG., editors. Anticarcinogenesis and Radiation Protection. Boston, MA: Springer US; 1988. p. 349-54.
36. Roberts W, Kartha M, Sagone AL Jr. Effect of irradiation on the hexose monophosphate shunt pathway of human lymphocytes. Radiation research. 1979; 79(3):601–10. [PubMed: 482615]
37. Lee JH, Kim SY, Kil IS, Park JW. Regulation of ionizing radiation-induced apoptosis by mitochondrial NADP+-dependent isocitrate dehydrogenase. The Journal of biological chemistry. 2007; 282(18):13385–94. [PubMed: 17350954]
38. Lee SM, Koh HJ, Park DC, Song BJ, Huh TL, Park JW. Cytosolic NADP(+)-dependent isocitrate dehydrogenase status modulates oxidative damage to cells. Free radical biology & medicine. 2002; 32(11):1185–96. [PubMed: 12031902]
39. Kim SY, Yoo YH, Park JW. Silencing of mitochondrial NADP(+)-dependent isocitrate dehydrogenase gene enhances glioma radiosensitivity. Biochemical and biophysical research communications. 2013; 433(2):260–5. [PubMed: 23500467]
40. Aird KM, Zhang G, Li H, Tu Z, Bitler BG, Garipov A, et al. Suppression of nucleotide metabolism underlies the establishment and maintenance of oncogene-induced senescence. Cell Rep. 2013; 3(4):1252–65. [PubMed: 23562156]
41. Pan J-S, Hong M-Z, Ren J-L. Reactive oxygen species: A double-edged sword in oncogenesis. World Journal of Gastroenterology: WJG. 2009; 15(14):1702–07. [PubMed: 19360913]
42. Lee JJ, Kim BC, Park MJ, Lee YS, Kim YN, Lee BL, et al. PTEN status switches cell fate between premature senescence and apoptosis in glioma exposed to ionizing radiation. Cell death and differentiation. 2011; 18(4):666–77. [PubMed: 21072054]
43. Dang L, White DW, Gross S, Bennett BD, Bittinger MA, Driggers EM, et al. Cancer-associated IDH1 mutations produce 2-hydroxyglutarate. Nature. 2009; 462(7274):739–44. [PubMed: 19935646]
44. Parsons DW, Jones S, Zhang X, Lin JC, Leary RJ, Angenendt P, et al. An integrated genomic analysis of human glioblastoma multiforme. Science (New York, NY). 2008; 321(5897):1807–12.
45. Yan H, Parsons DW, Jin G, McLendon R, Rasheed BA, Yuan W, et al. IDH1 and IDH2 mutations in gliomas. The New England journal of medicine. 2009; 360(8):765–73. [PubMed: 19228619]
46. Li S, Chou AP, Chen W, Chen R, Deng Y, Phillips HS, et al. Overexpression of isocitrate dehydrogenase mutant proteins renders glioma cells more sensitive to radiation. Neuro-oncology. 2013; 15(1):57–68. [PubMed: 23115158]
47. Chowdhury R, Yeoh KK, Tian YM, Hillringhaus L, Bagg EA, Rose NR, et al. The oncometabolite 2-hydroxyglutarate inhibits histone lysine demethylases. EMBO reports. 2011; 12(5):463–9. [PubMed: 21460794]
48. Lu C, Ward PS, Kapoor GS, Rohle D, Turcan S, Abdel-Wahab O, et al. IDH mutation impairs histone demethylation and results in a block to cell differentiation. Nature. 2012; 483(7390):474–8. [PubMed: 22343901]
49. Shi J, Zuo H, Ni L, Xia L, Zhao L, Gong M, et al. An IDH1 mutation inhibits growth of glioma cells via GSH depletion and ROS generation. Neurological science: official journal of the Italian Neurological Society and of the Italian Society of Clinical Neurophysiology. 2014; 35(6):839–45.

Author Manuscript Author Manuscript Author Manuscript Author Manuscript

50. Wang XW, Labussiere M, Valable S, Peres EA, Guillamo JS, Bernaudin M. IDH1(R132H) mutation increases U87 glioma cell sensitivity to radiation therapy in hypoxia. 2014; 2014:198697.

Author Manuscript
Author Manuscript
Author Manuscript
Author Manuscript

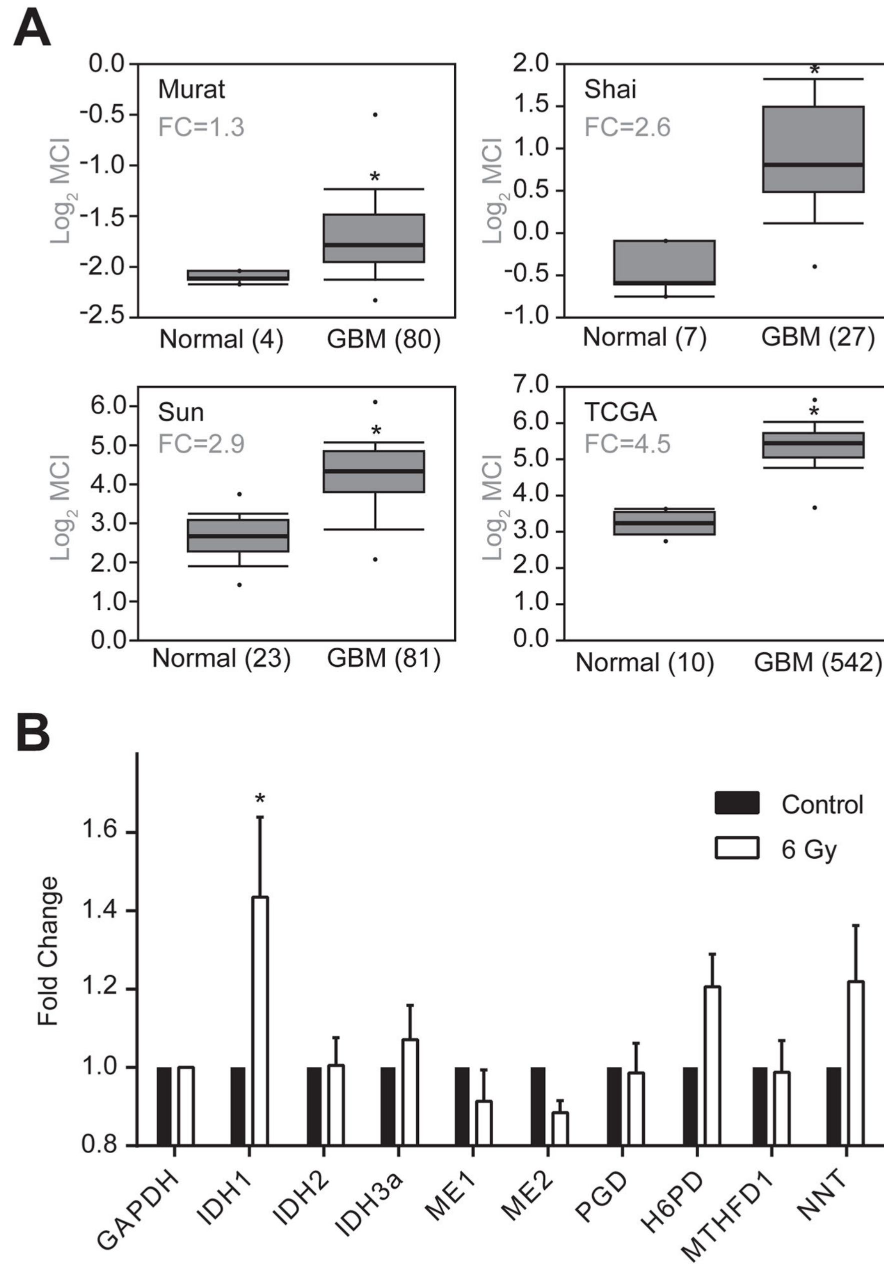


**Figure 1.**

IDH1 is upregulated in GBM and is further upregulated following radiation. **(A)** IDH1 transcript levels in GBM compared to normal brain tissue in datasets used in Table 1. Median-centered Intensity (MCI), Fold Change (FC). **(B)** Quantitative real-time PCR of NADPH-producing enzyme transcript levels in U87 GBM cells 24 h following 0 (black) or 6 Gy (white). Error bars represent the standard error of the mean (SEM) from n=6 biologic replicates. * $p<0.0001$.

Author Manuscript
Author Manuscript
Author Manuscript
Author Manuscript

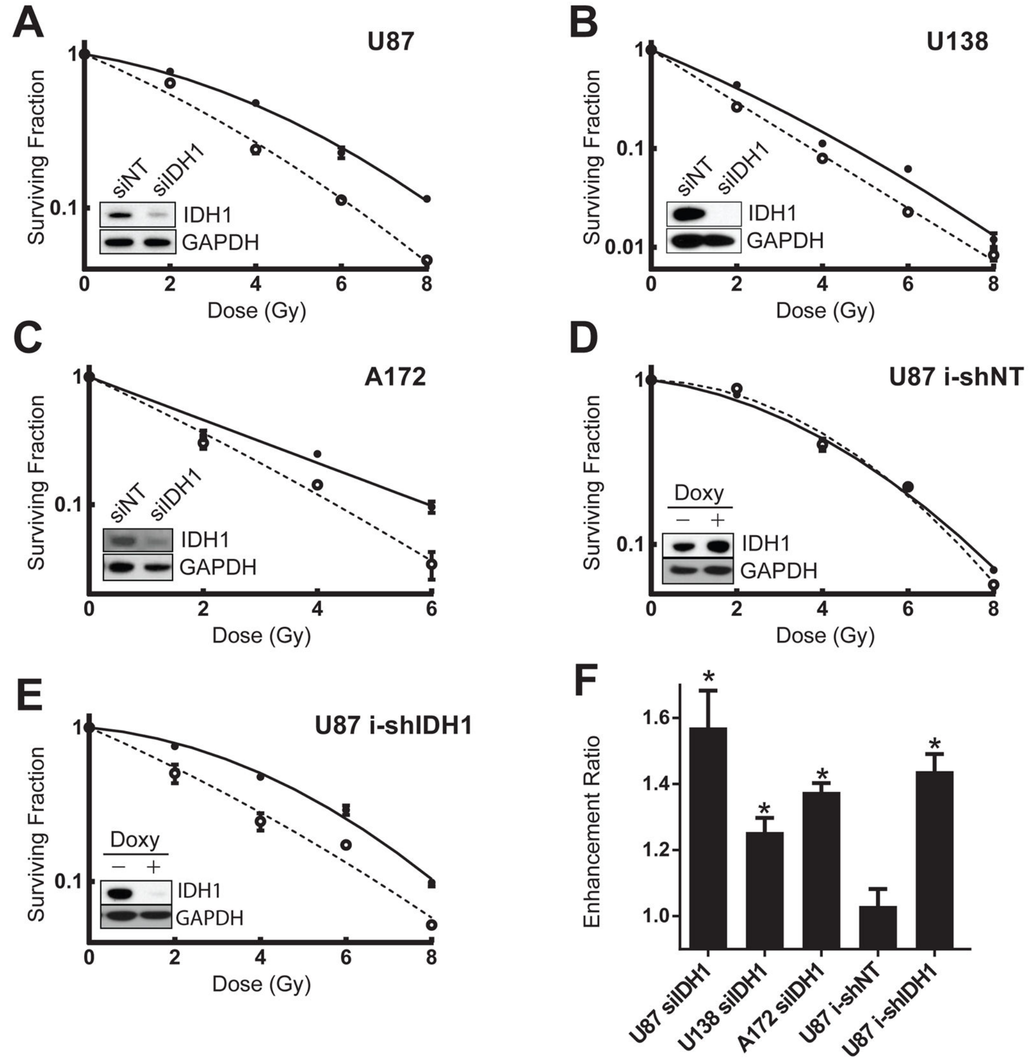


**Figure 2.**

Knockdown of IDH1 sensitizes GBM cell lines to radiation. **(A–C)** Three to four days following transfection with non-targeting (black circle) or IDH1 (open circle) siRNA, indicated GBM cell lines were irradiated and plated at clonal density and colonies were counted 10–14 days later. **(D and E)** U87 GBM cells carrying a doxycycline-inducible shRNA against IDH1 **(E)** or control **(D)** were treated with control media (black circle) or doxycycline-containing media (open circle) for 3–4 days, then irradiated and analyzed for colony formation as above. Curves depicted in **(A–E)** are representative of n=5 (U87), n=3 (U-138), n=3 (A172), n=3 (U87 i-shNT) or n=5 (U87 i-shIDH1) independent experiments. **(F)** Enhancement ratios were calculated for each condition based on the mean inactivating dose of radiation. * indicates $p < 0.05$ compared to control and error bars represent the SEM from 3–5 biologic replicates.

Author Manuscript Author Manuscript Author Manuscript Author Manuscript

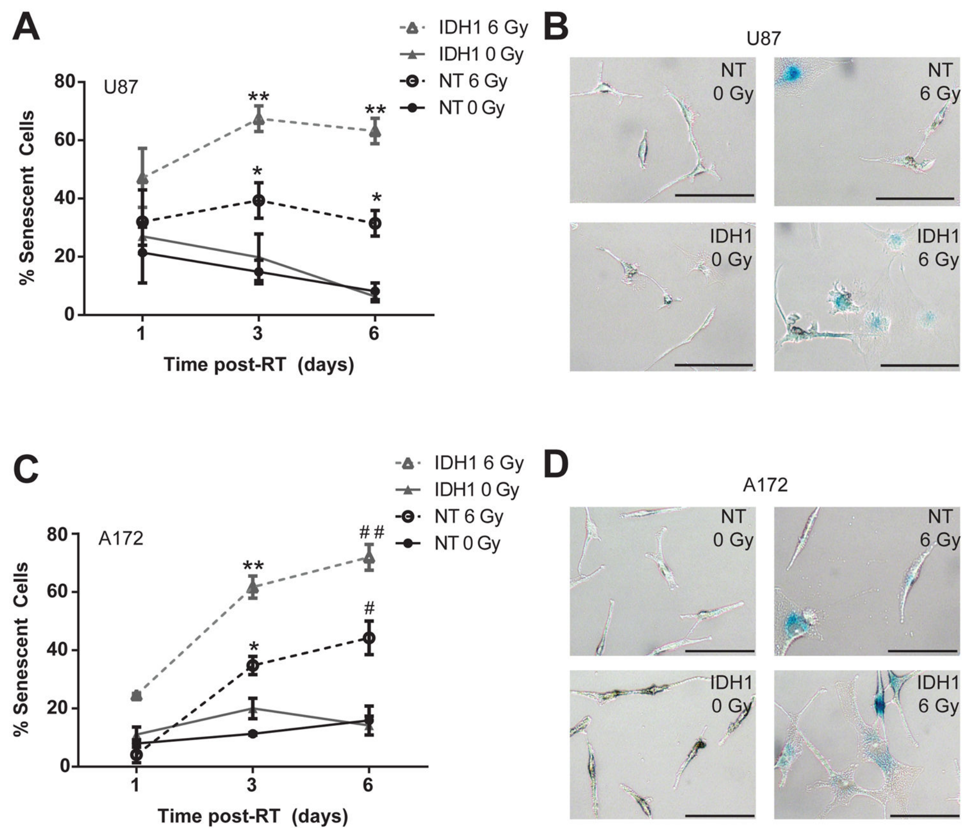


**Figure 3.**

IDH1 knockdown potentiates radiation-induced senescence in GBM. **(A)** U87 cells were irradiated with 6 Gy 3–4 days following transfection with NT or IDH1 siRNA. At 1, 3 or 6 days following RT, cells were stained and analyzed for senescence-associated β-galactosidase. Error bars represent the SEM from 4 independent biologic experimental replicates. * indicates $p<0.05$ compared to NT 0 Gy and ** indicates $p<0.05$ compared to IDH1 0 Gy and compared to NT 6 Gy. **(B)** Representative microscopy images of senescence-associated β-galactosidase staining of U87 cells treated with the indicated conditions 3 days following radiation. Scale bars are 100 μm. **(C)** A172 cells were irradiated with 6 Gy 3–4 days following transfection with NT or IDH1 siRNA. At 1, 3 or 6 days following RT, cells were stained and analyzed for senescence-associated β-galactosidase. Error bars represent the SEM from 3 independent biologic experimental replicates. * indicates $p<0.05$ compared to NT 0 Gy and ** indicates $p<0.05$ compared to IDH1 0 Gy and compared to NT 6 Gy. # indicates $p<0.1$ compared to NT 0 Gy and ## indicates $p<0.1$compared to IDH1 0 Gy and compared to NT 6 Gy **(D)** Representative microscopy images of senescence-associated β-galactosidase staining of A172 cells treated with the indicated conditions 3 days following radiation. Scale bars are 100 μm.

Author Manuscript Author Manuscript Author Manuscript Author Manuscript

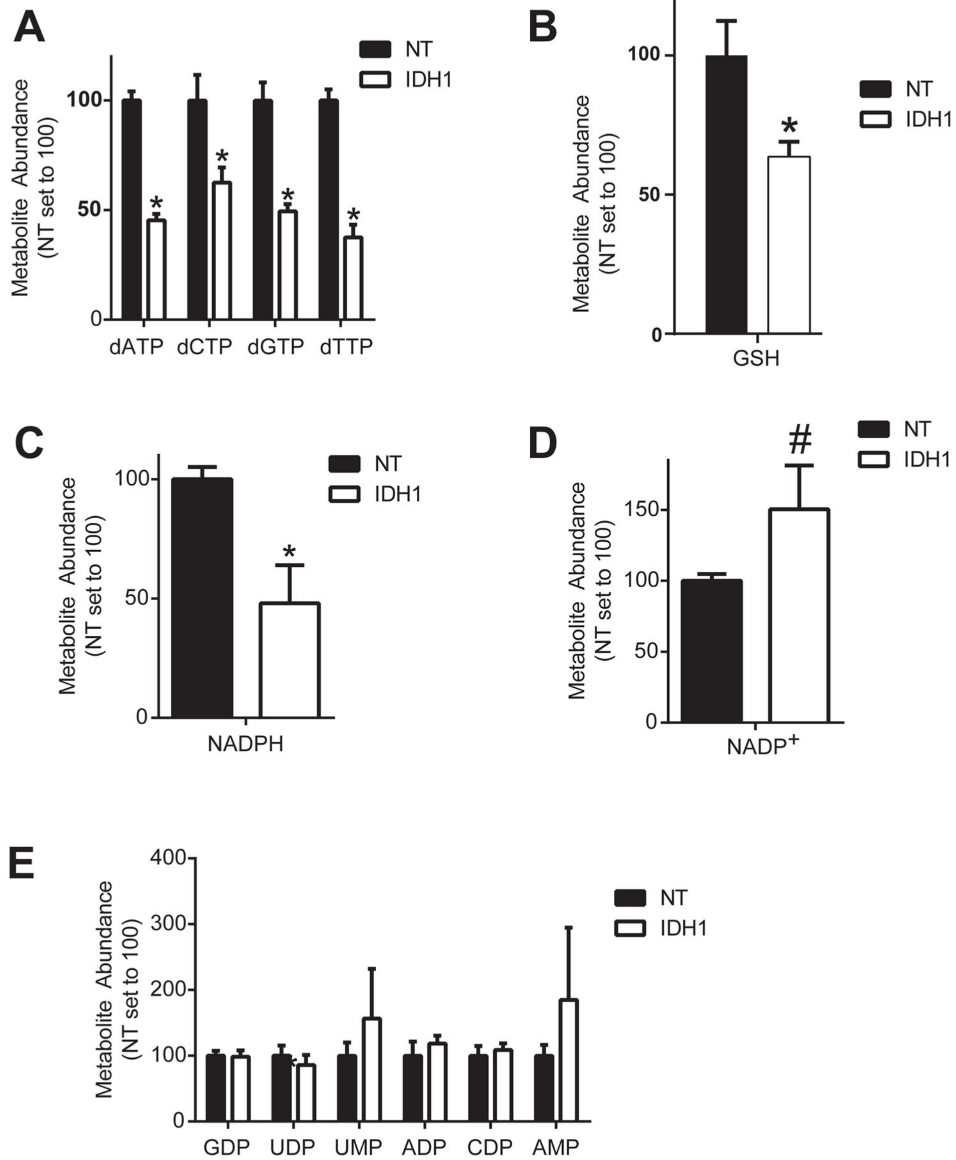


**Figure 4.**

IDH1 knockdown depletes antioxidant and deoxynucleotide pools in GBM. U87 cells were transfected with non-targeting (Black, NT) or IDH1 (White, IDH1) siRNA. After 3–4 days, cells were flash frozen and analyzed by mass spectrometry for **(A)** deoxynucleotides, **(B)** reduced glutathione, **(C)** NADPH, **(D)** NADP and **(E)** ribonucleotides. Error bars represent the SEM from between 3–7 independent determinations. * indicates p<0.05 and # indicates p=0.15.

Author Manuscript Author Manuscript Author Manuscript Author Manuscript

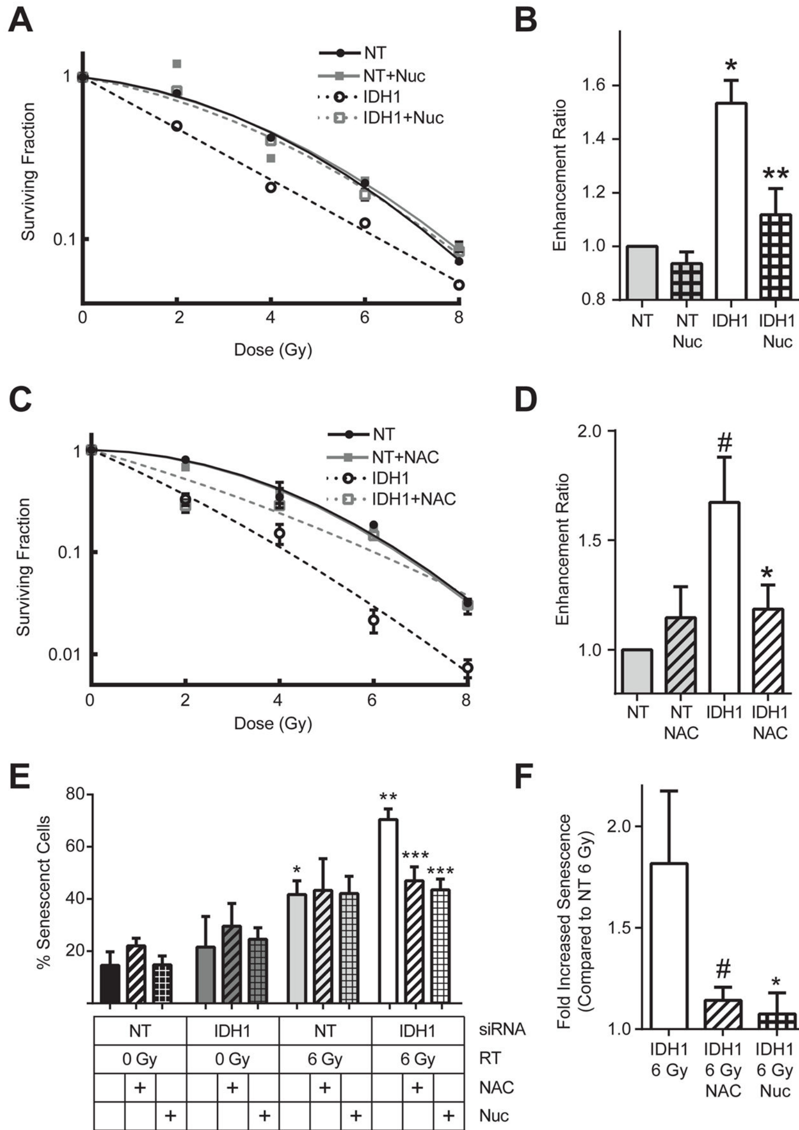


**Figure 5.**

Supplementation of NADPH-dependent metabolites rescues IDH1-mediated radiosensitization. **(A and B)** U87 cells were transfected with NT or IDH1 siRNA. After 3–4 days, cells were irradiated, plated at clonal density and analyzed for colony formation. Cells were incubated with control media or media containing 4x concentrated nucleosides (Nuc, EMD Millipore; 120 μM cytidine, guanosine, uridine, adenosine and 40 μM thymidine) for the 24 hours prior to and following radiation. **(A)** Single representative clonogenic survival assay of n=3 independent experiments performed. **(B)** Average enhancement ratios calculated from the mean inactivating dose of n=3 independent clonogenic survival assays. Error bars represent the SEM. * p=0.02 vs. NT. ** p=0.01 vs. IDH1. **(C and D)** U87 cells were transfected and treated as in (A and B) but incubated with control media or media containing 2 mM N-acetyl cysteine (NAC) for the 24 hours prior to and following radiation. **(C)** Representative clonogenic survival assay of n=3 independent experiments performed. **(D)** Average enhancement ratios calculated from the mean inactivating dose of n=3

independent clonogenic survival assays. Error bars represent the SEM. # p=0.06 vs. NT. * p=0.01 vs. IDH1. **(E and F)** U87 cells were irradiated with 6 Gy 3–4 days following transfection with NT or IDH1 siRNA and treated with the indicated rescue agent for the 24 hours before and after radiation as in (A and C). Three days following radiation, cells were stained and analyzed for senescence-associated β-galactosidase. Error bars represent the SEM from n=4 independent biologic replicates. **(E)** * p=0.02 vs. NT 0 Gy. ** p=0.03 vs. NT 6 Gy. *** p<0.05 vs. IDH1 Gy. **(F)** For each of the four experiments represented in (E), the % senescent cells was normalized to NT 6 Gy and plotted. # p=.054 vs. IDH1 6 Gy, ** p=0.01 vs. IDH1 6 Gy.

Author Manuscript Author Manuscript Author Manuscript Author Manuscript

Author Manuscript Author Manuscript Author Manuscript Author Manuscript

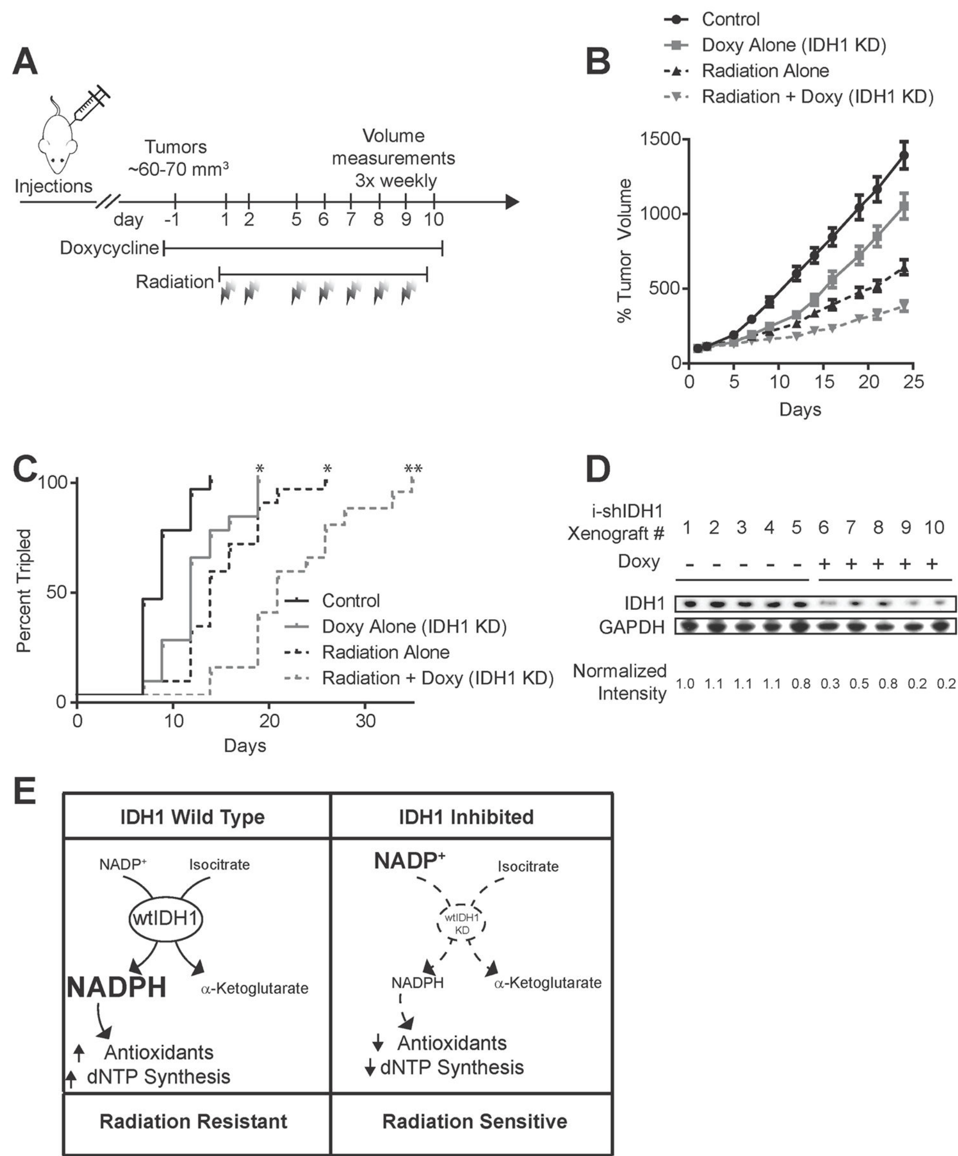


**Figure 6.**

IDH1 knockdown complements radiation to treat GBM xenografts. **(A)** U87 cells carrying a doxycycline-inducible shRNA against IDH1 were injected into flanks and tumors were allowed to form. Once tumors reached 60–70 mm$^3$, doxycycline water was initiated in appropriate groups. Two days following doxycycline initiation, radiation treatments began in appropriate groups with a total of 14 Gy administered in 7 fractions of 2 Gy each. Doxycycline was discontinued the day following radiation completion and tumor volumes were measured 3 times weekly. **(B)** Tumor volumes for the indicated treatment groups are normalized to the individual tumor sizes defined on day 1. Error bars show the SEM from 16 tumors from eight mice per group. **(C)** Kaplan Meier estimates of time to tumor tripling. Median times to tripling are 9 (control), 12 (doxycycline alone), 14 (radiation alone) and 21 (doxycycline+radiation) days. Tumor sizes are normalized to the size on the day of radiation initiation. * $p<0.005$ vs. control. ** $p<0.001$ vs. control, RT alone, and doxy alone. **(D)** Nine

Author Manuscript Author Manuscript Author Manuscript Author Manuscript

days following doxycycline initiation, xenografts were harvested, flash frozen and analyzed for IDH1 expression by immunoblot. Each band is from an individual tumor. **(E)** Metabolic model of IDH1-mediated radioresistance. In IDH1 wild type GBM, the enzymatic activity of IDH1 catalyzes the production of NADPH, which facilitates the maintenance of antioxidants and synthesis of deoxynucleotides, both of which abrogate the effects of radiation. When IDH1 is inhibited, antioxidant regeneration and deoxynucleotide synthesis are compromised increasing radiation sensitivity.

Author Manuscript

**Table 1**

IDH1 is the most upregulated NADPH-producing enzyme in GBM. Transcript levels of NADPH-producing enzymes were examined in 4 independent clinical datasets containing both GBM and normal brain. Within each clinical data set, individual NADPH-producing enzymes were ranked from most upregulated (#1) to least upregulated (#8).

| Overexpression rank of NADPH-producing enzymes | Sun | TCGA | Murat | Shai |
|---|---|---|---|---|
| 1 | **IDH1*** | **IDH1*** | 6PGD* | **IDH1*** |
| 2 | G6PDH* | 6PGD | **IDH1*** | MTHFD1 |
| 3 | 6PGD | G6PDH | MTHFD1 | ME2 |
| 4 | IDH2 | MTHFD1 | G6PDH | 6PGD |
| 5 | ME2 | IDH2 | ME2 | IDH2 |
| 6 | NNT | ME2 | IDH2 | NNT |
| 7 | ME1 | NNT | NNT | ME1 |
| 8 | MTHFD1 | ME1 | ME1 | G6PDH |

Enzymes denoted with * are among the top 5% of all upregulated genes associated with GBM in a given data set.